Statistical Assessment of Global and Local Cylinder Wear

Oscar Ruiz, *Member, IEEE,* and Carlos Vanegas, *Member, IEEE*

***Abstract*— Assessment of cylindricity has been traditionally performed on the basis of cylindrical crowns containing a set of points that are supposed to belong to a controlled cylinder. As such, all sampled points must lie within a crown. In contrast, the present paper analyzes the cylindricity for wear applications, in which a statistical trend is assessed, rather than to assure that all points fall within a given tolerance. Principal Component Analysis is used to identify the central axis of the sampled cylinder, allowing to find the actual (expected value of the) radius and axis of the cylinder. Application of k-cluster and transitive closure algorithms allow to identify particular areas of the cylinder which are specially deformed. For both, the local areas and the global cylinder, a quantile analysis allows to numerically grade the degree of deformation of the cylinder. The algorithms implemented are part of the CYLWEAR© system and used to assess local and global wear cylinders.**

I. Introduction

REGARDING extrusion or injection cylinders there is an economic interest in quantifying the degree of deformation away from a mathematical cylinder. The software processing a point sample of the interior of a cylinder is expected to fulfill the following criteria: (i) independence of the coordinate frame of the measurement, (ii) identification of the axis of the cylinder, (iii) identification and quantification of local, high wear areas, (iv) automated quantification of global wear.

The present article discusses a software that takes as input a point cloud evenly sampled on the interior wall of a cylinder and that is contained between two planes, approximately perpendicular to the cylinder axis. The point sample is assumed to be evenly spread in such an area, in such a manner that no part is over-sampled or under-sampled. No order is assumed in the point cloud.

II. Literature Review

An important application in metrology is the evaluation of cylindricity, since a large fraction of mechanical parts are cylinders. The evaluation of cylindricity is not simple, because it requires a number of circularity traces to be taken at different horizontal sections of the cylinder and must be combined with the straightness of the generators of the cylinder [1].

In the evaluation of cylindricity the zone cylinder has become a standard for the quality control community. The zone cylinder is the cylindrical crown contained between two co-axial cylinders with minimum radial separation (width) and containing all the data points. Determining the zone cylinder involves the calculation of the direction axis, and internal and external radius.

Sampling nominally cylindrical objects usually involves an apparatus consisting of a turntable, a probe, and the support of the probe. This measurement system involves three different axes: the axis of rotation of the table, the axis of the cylindrical object and the axis of the probe support [2]. In practice, these axes are not parallel, and accurate information of the orientation of the cylinder is not available. Therefore, the direction axis must be calculated.

A comparison of different methods for cylindricity evaluation is presented in [1]. An approach using normal least squares was introduced, which minimizes the squares of the perpendicular distances from the measured points to the axis of the cylinder. The author also presents a method based on the development of the surface of the cylinder, in which the surface is "flattened" using as reference the axis of the probe support. The flatness of the surface is then obtained from the mean plane equation.

Reference [2] presents a linear programming-based approach to estimate the minimum zone cylinder enclosing a set of points. The linear programming problem is iteratively solved in a 6-dimensional space generated by 6 parameters that define a hyperboloid associated to the cylinder. The above-mentioned approach is therefore relevant to the evaluation of overall cylinder deformation, but does not aim to solve the local wearing detection problem. The efficiency and accuracy of this method was improved through a procedure in which points that cannot provably define the solution are culled from the input point set [3].

The problem of finding the minimum width cylinder containing a set of points is an extension to three dimensions of the problem of finding the annulus of smallest width containing a set of points in the plane. Several works have addressed the minimum width annulus problem. Reference [4] proposes a fast algorithm that exploits the properties of convex-hull and Voronoi diagrams. Reference [5] proposes a generalized method for the minimum width annulus in a d-dimensional space. Reference [6] addresses this problem in 2-dimensions (disks) and 3-dimensions (balls). Their method for testing disk roundness (mentioned below) is extended to the evaluation of balls by partitioning them into several slices, each of which is evaluated as a disk.

Reference [7] also studies the problem of determining whether a manufactured cylinder is sufficiently round. They first introduce a procedure for testing roundness in disks, in which set of probes are iteratively taken at uniform intervals directed at the origin, using the finger probing model of [8]. The procedure stops when a decision is made on whether the sample points can be covered by some "thin" annulus. The roundness testing procedure is extended to cylinders by

Manuscript received January 15, 2007; revised March 15, 2007. This work was supported in part by EAFIT University, Medellin, COLOMBIA.

O. Ruiz (corresponding author) and C. Vanegas are with the CAD CAM CAE Laboratory at EAFIT University, Medellin, AA3300, COLOMBIA (phone: +57-4-261-9500 ext 521; fax: +57-4-266-4284; e-mail: oruiz,cvanega3@eafit.edu.co).

projecting the points on the surface of the cylinder onto the XY plane, and applying the "thin" annulus criterion to the projected points. Notice that this method assumes that the sampled cylinder is resting on the XY plane and that its orientation is known. As noted above, such an assumption is not always valid since the axes of the measurement system (e.g. the axis of rotation of the cylinder) are unknown in practice.

The problem of cylinder fitting is also addressed by [9], [10], as a part of their method for detecting bore holes for Industrial Automation. They propose a sequential cylinder parameter fitting in which the orientation of the axis is first calculated, followed by the calculation of the radius and the position of the axis. A previous step in this bore detection method consists in estimating the normal vector to the surface at each sampled point.

The first sub-quadratic solution to the minimum width cylindrical shell problem, based on a linearization of such problem, is presented in [11]. Again, the problem addressed is that of estimating the global deviation of a point set from a cylindrical shape, and does not cover our aim of statistical assessment.

General comments to the reviewed literature are: (i) a dimensional quality control problem is attacked, which poses the question of whether a workpiece must be rejected or not, (ii) the determination of minimal enclosing and maximal enclosed cylinders, minimum zone cylinder, etc. are sought, usually in cylinders which are placed in a particular position of the space, (iii) in the item (i), data are interpreted in literal way, i.e. ignoring the trends or statistical indicators of their quality. The approach undertaken in our work is to produce a statistical diagnose of the cylindricity (see section III-D), and therefore each data is taken as inherently biased by several sources of noise. One can do so, since our work is aimed to help the production manager to numerically evaluate the need to replace the cylinder when (from his/her point of view) the wear or distortion in the cylinder reaches unacceptable values (see section III-G). As a result, we do not use the typical deterministic geometry algorithms of the literature. Instead, we apply stochastic geometry to diagnose the data.

III. Methodology and Results

The diagnosis of cylinder wear is basically a treatment of an unordered point set, collected on the internal wall of the sampled cylinder. The point set is measured in the particular unknown (local) coordinate system of the reading instrument, different from the World Coordinate System -WCS- of the shop floor. Although the points are collected on a definite geometrical shape (a cylinder), the numerical values output by the measuring device contain several stochastic components.

The processing of the point cloud (see Figure 1) is as follows:

1) Assuming for the cylinder a Length/Diameter ratio larger than 5.0, a Principal Component Analysis -PCA- is run. The PCA allows to identify the direction of largest dispersion in the data, which is the direction of the cylinder axis. As a by-product, the center and mean radius of the cylinder are also identified.

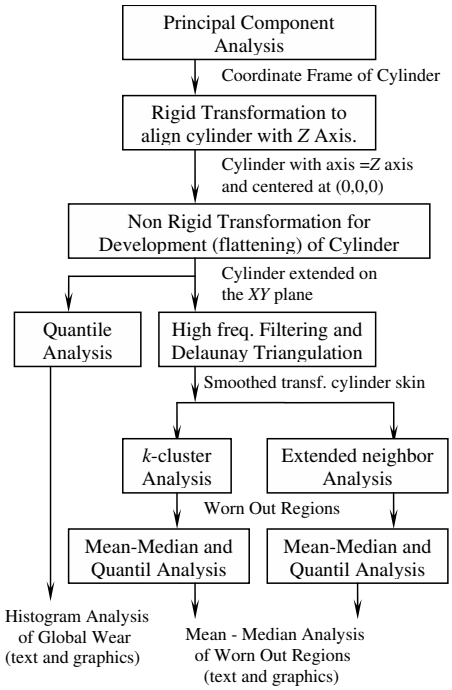

Fig. 1. Cylindricity Diagnose with Point Cloud

2) A rigid geometric transformation is applied to the point cloud to align the cylinder with the Z axis of the WCS.
3) A Quantile Analysis is performed, which renders the histogram of frequencies of radius deviations for the global point cloud.
4) The cylindrical data is developed (unwrapped or flattened) onto $\mathbb{R}^2$ (XY plane) to perform a local analysis.
5) A low pass filter is applied to the data, which eliminates the high frequencies of the point cloud.
6) A surface is reconstructed for the point data, using a lift of a Delaunay Triangulation, to facilitate the visual identification of the high wear areas. At this time, the data resembles a rectangular mountain region, whose heights correspond to the areas (regions of (θ, h) values) with larger cylinder wear.
7) Two alternative algorithms are applied to automatically identify such high wear areas: k-cluster and Extended Neighborhood Analyses.
8) Quantile and Mean-Median Analyses are performed on the local wear regions.
9) All the results are given in the form of text files (for documentation and analysis) and via graphic output (for the easy identification by the user).

A. Measured Data

Three sources of deviation of point data away of a perfect cylinder are assumed: (i) a general wear, (ii) localized wear spots, and (iii) measurement noise introduced by the scanner. The point set has an arbitrary orientation and position, and it is necessary to determine the coordinate system in which it was collected by the measuring devise. The nominal radius and length of the cylinder are assumed to be known.

B. Transformation of Measured Data to the World Coordinate System

The purpose of this section is to rigidly transform measured data so that the calculated axis of the cylinder is coincident with the Z axis of the WCS and its center is coincident with the origin O of the WCS. However, we know neither the axis of the cylinder, nor its effective radius and length. To determine such values is the purpose of the following section.

1) Principal Component Analysis: Let $P' = \{(x', y', z') \in \mathbb{R}^3\}$ be the set of points sampled on the surface of a cylinder $C(R, H, A, O)$, where R, H, A, O are the nominal radius, nominal length, axis and center of gravity of the cylinder, respectively. It must be noticed that only R and H are known. The actual values of radius, height, axis, and center must be determined from P'. By applying a Principal Component Analysis -PCA- the trends in the collected data will be identified (see [12], [13]).

Let Σ be the (3×3) covariance matrix of the process $P' = \{(x_1, y_1, z_1), \ldots, (x_n, y_n, z_n)\}$, with c_{ij} being the cross covariance of components i and j of the point set. Σ is semi-positive definite, since it is symmetric with non-negative main diagonal. The eigenvalues of Σ are non-negative real numbers λ_i. Then, Σ satisfies the equation $\Sigma.V = V.\Lambda$ with V a matrix whose columns are the (orthogonal) eigenvectors of Σ, and Λ is a diagonal matrix containing the eigenvalues of Σ. Without sacrificing generality one may sort the eigenvalues in decreasing order, say $\lambda_1 \geq \lambda_2 \geq \lambda_3 \geq 0$, and write the eigenpairs of the covariance matrix as:

$$\Sigma.V = \Sigma. \begin{bmatrix} v_1 & v_2 & v_3 \end{bmatrix} = \begin{bmatrix} v_1 & v_2 & v_3 \end{bmatrix} . \begin{bmatrix} \lambda_1 & 0 & 0 \\ 0 & \lambda_2 & 0 \\ 0 & 0 & \lambda_3 \end{bmatrix}$$

with λ_i being the variance of the data in the direction v_i. It follows that v_1 is the direction of the data P' in which maximal variance appears, v_2 is the direction in which the next decreasing variance appears, and v_3 is the direction with lowest data variance in P'. For a Length/Diameter ratio larger than 5.0, it can be seen that $v_1 \equiv A$, i.e. the axis of the cylinder A is the eigenvector associated with the largest eigenvalue or variance, λ_1 (the direction with highest variance of the data P'). Therefore $\Sigma.A = \lambda_1 A$. The triad v_1, v_2, v_3 is orthogonal, and we may enforce the condition $v_1 \times v_2 = v_3$, forming a right handed canonical coordinate system. Notice that given the cylindrical symmetry of the data, the second and third variances are almost the same. Except for numeric stochastic errors: $\lambda_2 \approx \lambda_3$.

2) Transformation to a standardized coordinate system: Once we know the axis $A = (A_x, A_y, A_z)$ and the center of mass $O = (O_x, O_y, O_z)$ of the measured cylinder, we must find out a 4×4 rigid transformation

$$M = \begin{bmatrix} R^*_{3\times3} & T^*_{3\times1} \\ 0 \quad 0 \quad 0 & 1 \end{bmatrix}$$

to move the point data in such a way that the axis of the cylinder is coincident with the Z axis of the WCS, and its center of mass is coincident with the origin of the WCS.

$$\begin{bmatrix} R^* & T^* \\ 0 \quad 0 \quad 0 & 1 \end{bmatrix} = \begin{bmatrix} v_2 & v_3 & A & O \\ 0 & 0 & 0 & 1 \end{bmatrix}^{-1} \quad (1)$$

Once R^* and T^* have been determined from (1), each point sampled can be transformed with (2), so the data set looks like in Figures 2(a) and 2(b).

$$\begin{bmatrix} x \\ y \\ z \\ 1 \end{bmatrix} = \begin{bmatrix} R* & T* \\ 0 \quad 0 \quad 0 & 1 \end{bmatrix} . \begin{bmatrix} x' \\ y' \\ z' \\ 1 \end{bmatrix} \quad (2)$$

C. Mapping of Normalized Cylinder 3D data onto 2D

After a normalization has been performed on the measured data, the axis of the cylinder coincides with the Z axis, and its center of mass with the origin O. The next step is to "unwrap" the point cylinder, and to extend the point set on the XY plane. The function used to do so is not an isometry, since the cylinder data is shrunk in order to fit into a rectangular basis of size 1.0×1.0.

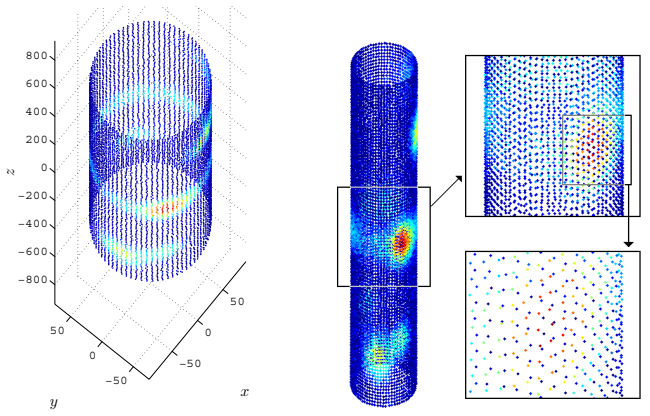

(a) Transformation of general measured point set to bring cylinder axis to Z axis

(b) Detail of the point set with local damage on cylinder surface

Fig. 2. Sampling of a cylinder surface with local damage

The point set $P = \{(x, y, z)\}$ (which is the cylinder point sample with its axis aligned with the Z axis of the World Coordinate System) is transformed into a new set $Q = \{(x_f, y_f, z_f)\}$, with the following characteristics: (i) the z_f coordinate of each point in Q is the deviation, for the corresponding point in P, away from the calculated radius of the cylinder, (ii) the point set Q is organized as a function $g : \mathbb{R}^2 \rightarrow \mathbb{R}$, with $z_f = g(x_f, y_f)$, (iii) the (x, y) pairs are included in a rectangular domain in $\mathbb{R}^2$. This means, the cylinder has been unwrapped and extended on the XY plane (Figure 3). The unwrapping transformation for set P into Q is described in equation (3). It maps each point (x, y, z) sampled on the surface of a cylinder into (x_f, y_f, z_f) with $(x_f, y_f) \in [-0.5, 0.5] \times [-0.5, 0.5]$.

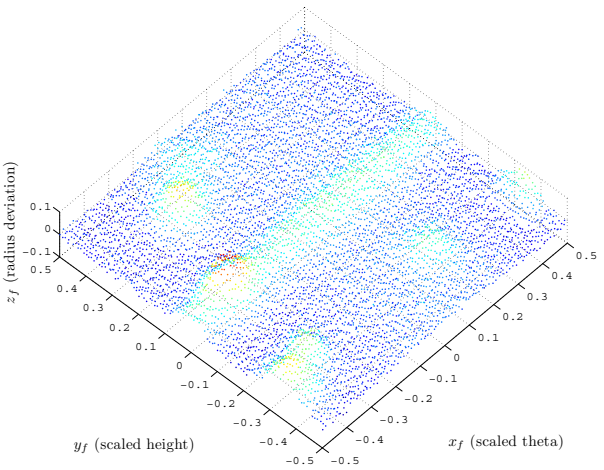

Fig. 3. Point set with noise, placed in general position in space. Measured data in an experiment.

$$\begin{aligned} x_f &= \frac{\arctan(x,y)}{2\pi} - \frac{1}{2} \\ y_f &= \frac{1}{2}\left(\frac{z}{\max(|\max_i z_i|, |\min_i z_i|)}\right) \\ z_f &= \|(x,y)\| - R \end{aligned} \tag{3}$$

The reader may notice that in Figure 3 the intensity is not uniform. This is due to the fact that a color coding is given to the z_f coordinate. Consequently, regions with larger deviation from the nominal radius (regions with higher wear) look lighter in the image.

D. Statistical Analysis

The points in Figure 3 have a z_f coordinate that represents the deviation with respect to the nominal cylinder radius. This deviation is due to three causes: (i) a general wear of the cylinder, (ii) localized wear in specific regions of the cylinder, and (iii) a stochastic noise resulting from the measurement process. The purpose of this step is to measure the deviation of the data that is explained by each factor, i.e. how much in the collected data are these components present. Figure 4 shows the histogram of frequencies with respect to z_f. The horizontal axis is divided into intervals of the z_f variable. The vertical values correspond to the number of points whose radial deviation z_f falls within each interval. In this histogram we can see in the range $[-0.02, 0.02]$ an approximately normal distribution with mean $\mu = 0$. This distribution corresponds to the sampling error of the instrument (factor (iii) above). Above a deviation of 0.02 away from the nominal radius we find the effects (i) and (ii) mentioned before. Thus, in the interval $[0.02, 0.07]$ one will find the cutting deviation to classify localized wear or damage in the cylinder.

By using the frequency histogram of Figure 4, one is able to separate the set of points Q into points showing only overall wear vs. points showing overall and localized wear. In the histogram, the cutting value is $\varepsilon = 0.02$. This means, points whose radial deviation is below 0.02mm are considered to have overall wear. Points with radial deviation above 0.02mm are considered to present overall and localized wear. These points constitute the set Q_ε.

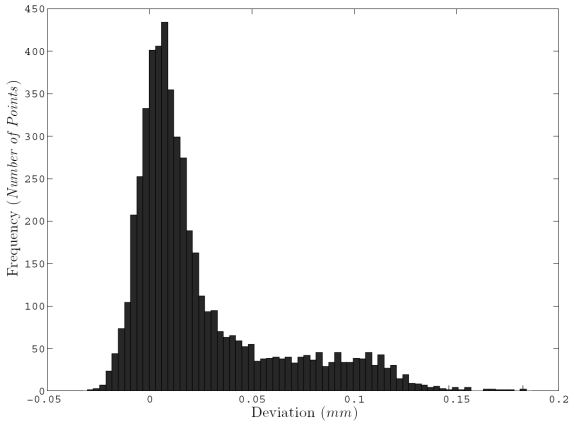

Fig. 4. Histogram of the cylinder radius deviation.

E. Cluster Analysis

The purpose of the cluster analysis applied to a set of n points in $\mathbb{R}^m$ is to identify k groups (k being set by the user) in the n points, such that in each group the points are close to each other, and at the same time far away from the points in other groups. In this manner, in the initial population, k clusters of neighboring points are identified. Let the population be formed in this application by n points in the set Q_ε. The space of the points is $\mathbb{R}^m = \mathbb{R}^3$. Let each point q_i in Q_ε be noted as:

$$(x_{fi}, y_{fi}, z_{fi}) = (X_{i,1}, X_{i,2}, X_{i,3}) \in Q_\varepsilon$$

The mean of the j-th variable ($j = 1, 2, 3$) in the l-th group is noted by $\bar{X}_{(l),j}$, for $l = 1, \ldots, k$. The distance of the point q_i to the l-th cluster is:

$$D_{(i,l)} = \left[\sum_{j=1}^{3} (X_{i,j} - \bar{X}_{(l)j})^2\right]^{1/2}$$

The error of the partition is given by the summation of the distance of each point to the cluster under which it is classified. The error of a partition $P(n,k)$ of the n points in k clusters is noted by:

$$\varepsilon(P(n,k)) = \sum_{i=1}^{n} [D_{(i,l(i))}]^2$$

where $l(i)$ is the set under which the i-th point is classified, which is the one for which the distance $D(i,l)$ is a minimum. It must be noticed that for each partition of the set Q_ε there will exist a value $\varepsilon(P(n,k))$. The partition that makes $\varepsilon(P(n,k))$ a minimum is our k-mean partition.

The method of the k-means is summarized as follows:

1) Propose k initial points $\bar{X}_{(l)}$.
2) For each point q_i find out its corresponding cluster $l(i)$ (for which the summation of the $D(i,l)$ is a minimum).
3) Recalculate $\bar{X}_{(l)}$ as the centroid of the q_i points belonging to the cluster $l(i)$.
4) Repeat the steps 2 and 3 until $l(i)$ remains constant for every i between successive iterations. At this point, $\varepsilon(P(n,k))$ reaches a minimum.

In this manner the points migrate from one cluster to another, until the reduction of $\varepsilon(P(n,k))$ is zero. After the $l(i)$ are found with the previous algorithm, and as a visualization aid, the convex hull of each $l(i)$ may be found and drawn. In the particular case of the wear of the cylinders, such a visual post-processing helps in displaying the zones of the cylinder whose wear is higher. The main inconvenience of the k-means method is the need of pre-establishing k, the number of clusters. For this reason an alternative method is introduced next.

F. Partition Analysis

The set Q_ε in (4) represents all the point data whose distance to the axis of the cylinder is higher than the threshold. Notice that the proposed algorithm seeks to eliminate the user interaction and to identify and bound the different deformation regions. Therefore, Q_ε must be partitioned into the local zones that present a particular wear of the cylinder. For such a purpose we define an equivalence relation R on Q_ε and then we calculate a partition Π of Q_ε by R. Let R be the equivalence relation defined as:

$$R(a,b) \Leftrightarrow \exists q_1, q_2, ..., q_w((q_i \in Q_\varepsilon, i = 1, ..., w) \wedge (a = q_1) \wedge (b = q_w) \wedge (\|q_i - q_{i+1}\| < \delta)) \quad (4)$$

This equivalence relation basically states that points a and b belonging to Q_ε are equivalent if and only if there exists a path of points starting at a and ending at b such that two points q_i and q_{i+1} of the path are not separated from each other by more than a distance δ. In order to partition Q_ε in a partition of all points that are equivalent to each other, we apply algorithm 1.

Algorithm 1 Partitioning Algorithm to calculate neighborhoods of cylinder deformation

```
Π = []
while Q_ε do
    p = first(Q)
    queue_to_expand = {p}
    Q_ε = Q_ε − {p}
    partition = {}
    while queue_to_expand do
        element_to_expand = first(queue_to_expand)
        partition = partition ∪ {element_to_expand}
        queue_to_expand = queue_to_expand − {element_to_expand}
        for a such that R(element_to_expand, a) do
            Q_ε = Q_ε − {a}
            queue_to_expand = queue_to_expand ∪ {a}
        end for
    end while
    Π = [Π, partition]
end while
```

Figure 5 shows the results of the partition algorithm applied on $Q = Q_{0.02}$. The three resulting data sets are automatically classified by the algorithm, projected on the XY plane, and the convex hull of the projection calculated and displayed on such a plane in Figure 5.

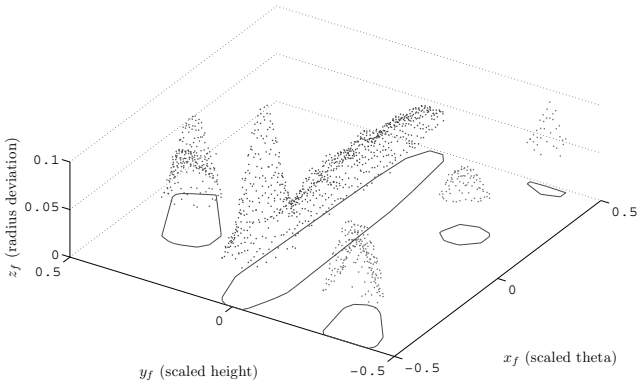

Fig. 5. Result of localized deformations found with partition analysis.

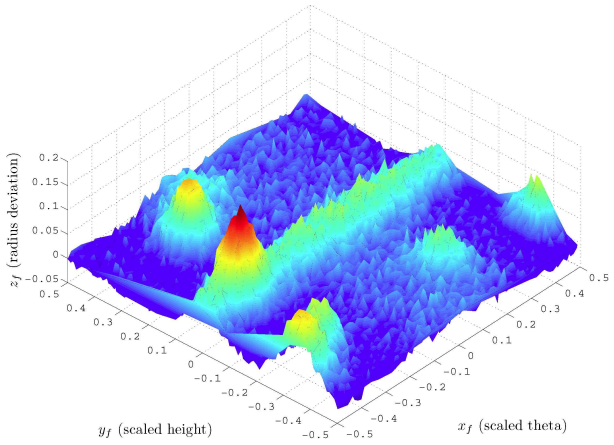

Fig. 6. Surface of Radius deformation with physical dimensions (workpiece coordinate system)

Figures 6 and 7 present the different noise factors in the flattened data set. Figure 6 shows the unfiltered data set in the scaled dimensions of the cylinder, while figure 7 shows the filtered data set mapped back to the physical dimensions of the cylinder. The localized damage in this data set has the shape of a mountain ridge (typical of a case in which a foreign object slides inside the cylinder) accompanied by isolated peaks. The highest deformation is present in a region centered in point $h = 500$mm and $\theta = 60^o$. Also, the wear located at $[0^o, 100]$ is the same as the one located at $[360^o, 100]$, since $0^o = 360^o$ because the cylinder wraps itself.

G. Diagnose Output

Three different outputs are produced from the process previously discussed: (i) graphical; (ii) histograms of frequency of radial deformation; and (iii) output file. They are discussed next.

1) Graphical Output: The radial deformation is converted to a function $f : \Theta \times H \rightarrow \Delta R$ (the deviation of the radius form its nominal value, see Figure 6). Delaunay triangulations and filtering are applied to display such a surface, as well as the regions of $f : \Theta \times H$ which represent a higher ΔR. Colors

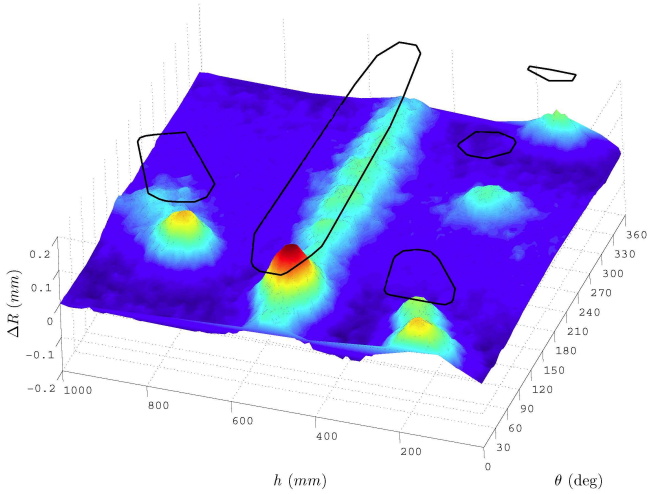

Fig. 7. Filtered, automatically-detected localized Wear Regions (using Partition Analysis)

green and blue mean lower deformation, while colors yellow and red indicate higher deformation.

2) Histogram of Frequencies of Radial Deformation: A histogram results from plotting the number of samples n_i measured which fall into each range of radius deviation $(\Delta(R_i))$ (Figure 4). Two clearly differentiated regions appear: (i) A normal distribution of measurement errors, centered in 0, containing negative values of ΔR. Values of ΔR between $[-\sigma, +\sigma]$ correspond to the measurement errors; and (ii) Values of ΔR above σ representing the deterministic trend of the data, which corresponds to the wear.

3) Output File: The output file contains two basic components: (i) the quantile information for the *global deformation* of the cylinder radius (ΔR deviation from the nominal radius); and (ii) the statistical information for each one of the *local areas of higher wear*. Global information corresponds to a text version of the histogram information discussed above. Local deformation includes for each area of large deformation the mean, median, standard deviation, maximal deviation and position of the wear area (θ, h).

IV. Conclusions and Further Work

This article has presented a software tool to diagnose the general and local wear of a cylinder. No assumption is made on the orientation or position of the cylinder in the space, or on the coordinate frame of the measuring devise. The software implemented is successful in identifying the position in space of the cylinder (in this case, five degrees of freedom). These algorithms filter out high frequencies in the data, fit a surface to the resulting point cloud, and identify by two alternative methods the regions of largest local wear. Several statistical reports (quantile and frequency histogram) are produced, which also diagnose the cylinder in local spots as well as globally.

Future efforts include:

1) Bringing the devised tools to the domain of dimensional quality control.
2) Approaching the problem as a non linear minimization or optimization one.
3) Using the findings in the previous item to diagnose other geometries different from the cylindrical one (torus, spheres, partial cylinders, cones, etc.).

References

[1] T. S. R. Murthy, "Comparison of different algorithms for cylindricity evaluation," Int. J. Mach. Tool Design & Res., vol 22, no. 4, pp. 283-292, 1982.
[2] O. Devillers, and F. P. Preparata, "Evaluating the cylindricity of a nominally cylindrical point set," in Proc. 11th Annual ACM-SIAM Symposium on Discrete Algorithms, Philadelphia, PA, 2000, pp. 518-527.
[3] O. Devillers, and F. P. Preparata, "Culling a set of points for roundness or cylindricity evaluations," Int. J. Comput. Geom. Appl, vol. 13, no. 3, pp. 231-240, 2003.
[4] U. Roy, and X. Zhang, "Establishment of a pair of concentric circles with the minimum radial separation for assessing rounding error", Computer Aided Design, vol. 24, no. 3, pp. 161-168, 1992.
[5] J. Garcia, and P. A. Ramos, "Fitting a set of points by a circle," in Proc. ACM Conference on Computational Geometry, 1997, pp. 139-146.
[6] P. Bose, and P. Morin, "Testing the quality of manufactured disks and balls," Algorithmica, vol. 38, no. 1, pp. 161-177, Oct. 2003.
[7] P. Bose, and P. Morin, "Testing the quality of manufactured disks and cylinders," in Proc. 9th international Symposium on Algorithms and Computation, Lecture Notes in Computer Science, vol. 1533, K. Chwa and O. H. Ibarra, Eds. London: Springer-Verlag, 1998, pp. 129-138.
[8] R. Cole, and C. K. Yap, "Shape from probing," Journal of Algorithms, vol. 8, no. 1, pp. 19-38, Mar. 1987.
[9] G. Biegelbauer, and M. Vincze, "Fast and robust bore detection in range image data for industrial automation," in Proc. 2nd international Symposium on 3D Data Processing, Visualization, and Transmission, Washington, DC, 2004, pp. 526-533.
[10] G. Biegelbauer, and M. Vincze, "3D vision-guided bore inspection system," in Proc. 4th IEEE international Conference on Computer Vision Systems, Washington, DC, 2006.
[11] S. Har-Peled, and K. R. Varadarajan, "Approximate shape fitting via linearization," in Proc. 42nd Annual IEEE Symposium Found. Comp. Sci., 2001, pp. 66-73.
[12] O. E. Ruiz, C. A. Cadavid, M. J. Garcia, and R. Martinod, "Principal component analysis -PCA- and Delone triangulations for PL approximation C1-continuous 1-manifolds in Rn," in Proc. Computer Graphics and Imaging (CGIM), Kauai, HI, August 17-19, 2004.
[13] O. E. Ruiz, and C. A. Vanegas, "Piecewise linear curve reconstruction from point clouds," in Proc. 6th International Symposium series on Tools and Methods of Competitive Engineering, Ljubljana, Slovenia, April 18-22, 2006, pp 285-298.

Associate Professor Oscar E. Ruiz was born in 1961 in Tunja, Colombia. He obtained B.Sc. degrees in Mechanical Eng. (1983) and Computer Science (1987) at Los Andes University, Bogotá, Colombia, a M.Sc. degree with emphasis in CAM (1991) and a Ph.D. with emphasis in CAD (1995) from the Mechanical & Industrial Eng. Dept. of University of Illinois at Urbana-Champaign, USA. Dr. Ruiz has held Visiting Researcher positions at Ford Motor Co. (Dearborn, USA. 1993, 1995), Fraunhofer Inst. Graphische Datenverarbeitung (Darsmstad, Germany 1999, 2001), University of Vigo (1999, 2002), Max Planck Institute for Informatik (2004). In 1996 Dr. Ruiz was appointed as Faculty of the Mechanical Eng. and Computer Science Depts. at EAFIT University, Medellin, Colombia, and has been ever since the coordinator of the CAD/CAM/CAE Laboratory. His interests are Computer Aided Geometric Design, Geometric Reasoning and App. Comp. Geometry.

Carlos A. Vanegas will obtain his B.Sc. degree in Applied Mathematics at EAFIT University, Colombia, in June 2007. He has been a research assistant at the CAD/CAM/CAE Laboratory since 2004, and has held Visiting Research Assistant positions in the University of Vigo, Vigo, Spain, in 2005 and 2006. His research interests are Computational Geometry and Computer Graphics.